Development of Composite Load Models of Power Systems using On-line Measurement Data

Byoung-Kon Choi*, Hsiao-Dong Chiang*, Yinhong Li*, Yung-Tien Chen**
Der-Hua Huang*** and Mark G. Lauby*****

Abstract - Load representation has a significant impact on power system analysis and control results. In this paper, composite load models are developed based on on-line measurement data from a practical power system. Three types of static-dynamic load models are derived: general ZIP-induction motor model, Exponential-induction motor model and Z-induction motor model. For the dynamic induction motor model, two different third-order induction motor models are studied. The performances in modeling real and reactive power behaviors by composite load models are compared with other dynamic load models in terms of relative mismatch error. In addition, numerical consideration of ill-conditioned parameters is addressed based on trajectory sensitivity. Numerical studies indicate that the developed composite load models can accurately capture the dynamic behaviors of loads during disturbance.

Keywords: composite load model, measurement-based approach, nonlinear least-squares, parameter estimation, stability analysis

1. Introduction

The accuracy of stability analysis findings has a significant impact on the quality of power system operational guidelines, operational planning, and design. The accuracy of stability analysis, however, largely depends on the validity of system models employed in describing power system dynamic behaviors. Effective system models are essential for simulating complex power system behaviors. Load characteristics are known to have a significant impact on power system dynamics. Inaccurate load models, for instance, can lead to power system operation in modes that result in actual system collapse or separation [1].

Until now standard model structures for loads are still unavailable while several IEEE standard model structures have been proposed for synchronous generators [2], and excitation systems [3]. Despite the fact that several load models have been proposed, they appear to be adequate for some types of power system dynamic analysis, but not for others. The need for the development of accurate dynamic load models for certain types of power system dynamic analysis remains strong. Load modeling includes two tasks: deriving a suitable model structure for a load bus, and obtaining values of the associated model parameters [4]. Currently, there are four favored methods for deriving a load model structure: physically-based method, component-based method, artificial neural-network (ANN)-based method [5], and hybrid method (combination of the above three methods).

Once the model structure is determined, the remaining issue is how to estimate parameter values. Two approaches are available to estimate load model parameters: the component-based approach and the measurement-based approach [4, 19]. Component-based load modeling is to derive model parameters by aggregating models of the individual components. This approach requires gathering load class mix, load composition data and the dynamical behaviors of each load component [4]. The measurement-based approach involves placing measurement systems at load buses for which load models will be developed. This approach has the advantage of direct measurement of the actual load behaviors during system disturbances so that accurate load models can be obtained directly in the form needed for the inputs of existing power system analysis and control programs [4, 6]. Because of the attractive features offered by the measurement-based approach, an on-line transient data recording system has been developed at the Taipower company to investigate actual load behaviors during system disturbances [7, 8].

At each substation, power system loads represent the aggregation of hundreds or thousands of individual component devices such as motor, lighting, and electrical appliances. Load models aim to represent their aggregate behaviors. Several composite load model structures have

* School of Electrical and Computer Engineering, Cornell University, Ithaca, NY 14853 USA. (bkc7@cornell.edu)
** System Planning Department, Taiwan Power Company, Taipei, Taiwan, R.O.C.
*** EPRI, Palo Alto, CA 94303 USA.
Received December 13, 2005 ; Accepted February 28, 2006

been proposed based on the physical insights of load composition and load behavior at each substation [6, 9-13]. For example a (linear) dynamic ZIP-motor load model was developed based on field measurement data [6]. In this model, the static ZIP portion of the load is represented by a combination of constant impedance (Z), constant current (I), and constant power (P) components, and it is slightly different from the general form while the dynamic load is represented by a third-order induction motor model.

In this paper, three composite load models are developed based on on-line measurement data from the Taipower system: general ZIP-induction motor (GZIP-IM) load model, exponential-induction motor (Exp-IM) load model, and Z-induction motor (Z-IM) load model. The GZIP-IM load model is a combination of static load, which consists of a general ZIP model structure [19], and dynamic load, which is a third-order induction motor model structure. The static part of the Exp-IM load model is represented by a static exponential model while the dynamic part is the same as that of GZIP-IM model. In the Z-IM load model, a different type of a third-order induction motor model, say, internal voltage form, can be used while the static load is of constant impedance.

The parameters of the three composite load models are estimated based on on-line measurement data. The task of load model parameter estimation is formulated as a nonlinear least squares problem with the output mismatch error as the objective function. The performances of three composite load models are evaluated in terms of estimation relative error.

2. Preliminary of Measurement-based Approach

When a (credible) system disturbance occurs, the system at each substation is triggered to record the three-phase currents and voltages and store the data on a local computer. At present, nine sets of self-acting monitoring systems are installed at the level of primary substations and distribution substations of the Taipower system [7]. Currently, 18 trigger types such as voltage level violation and frequency limit violation are defined in the system. The Discrete Fourier Transformation (DFT) technique is used to transform the recorded data into phasor form. The voltage and current phasors at each substation are then used to compute real and reactive power at the substation. The recorder system records signals that correspond to voltage variations from about 0.5 to 1.2 p.u., current variations from 0.1 to 1.0 p.u., and frequency variations from 55 to 65 Hz [6]. The sampling rate of the data recorder system can be flexibly adjusted and the sampling rate of measurement data in our studies was about 3840 Hz per channel (16 channels in parallel) with all channels being sampled at the same frequency.

The real and reactive powers are calculated from the computed symmetrical components of voltages and currents using the positive sequence method. Then we test the adequacy of the calculated input-output data based on appropriate data selection guidelines in order to drop out the data that may not contain sufficient information for parameter estimation. A procedure for identifying a composite load model based on measurement data is described as follows:

Step 1. Obtain a set of input-output data derived from a set of measurements.
Step 2. Select a composite load model structure.
Step 3. Estimate its parameters using a suitable method and estimation criterion.
Step 4. Evaluate the derived model using the estimation criterion.
Step 5. If criterion is not met, take remedial actions; for example, attempt another estimation method, or attempt another model structure and go to Step 3.

In Step 1, we use calculated positive sequence voltage magnitude (V) and possibly frequency variation as input and use computed real, reactive powers (P, Q) as output. By the very nature of the problem, the true parameter values are unknown and it is unrealistic to define a direct parameter error. We instead define an output error function that can be computed from measurement output and model output. In Step 3, since measurements are usually taken at discrete instances, this indicates the necessity of deriving a discrete-time space model when the original model is expressed as a continuous state space model. Discretization of linear dynamic model is quite straightforward. A few transformation methods between the s - domain and the z -domain are available; for example, the well-known forward rectangle rule or backward rectangle, or Tustin transformation can be applied.

One key objective for composite load model identification is to develop an accurate load model in which the model output is as close to the measured output as possible; making the so-called relative error between the measured output and the model output as small as possible.

3. Composite Load Model Structures

A composite load model structure consists of a static part and a dynamic part. In this section, we will derive useful system representation for three linear composite load models: GZIP-IM load model, Exp-IM load model and Z-IM load model. The static load part of each composite load model is connected with the third-order induction motor in parallel. The overall composite load model is described by

a set of differential-algebraic equations [6]:

$$\begin{aligned} \dot{x}_r &= g(x_r, u, p) \\ y &= h(x_r, u, p) \end{aligned} \tag{1}$$

where $g(\cdot,\cdot,\cdot)$ and $h(\cdot,\cdot,\cdot)$ are nonlinear functions of the state variable x_r, input u and the parameter vector p.

A. GZIP-Induction Motor Load Model

A schematic of the composite equivalent circuit for the GZIP-IM load model is shown in Fig. 1.

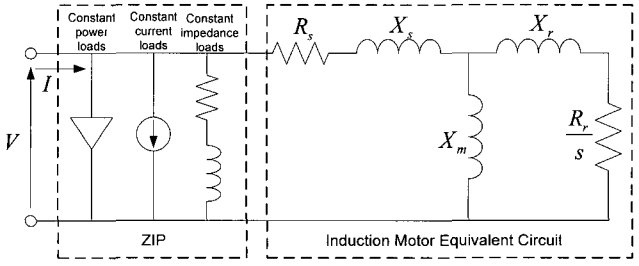

Fig. 1. A schematic of the GZIP-induction motor model

The static part of the GZIP-IM model is represented by a form of polynomial function of bus voltage and given by (2), (3):

$$P_{ZIP} = P_{ZIP0}\left[p_1 (V/V_0)^2 + p_2 (V/V_0)^1 + p_3\right] \tag{2}$$

$$Q_{ZIP} = Q_{ZIP0}\left[q_1 (V/V_0)^2 + q_2 (V/V_0)^1 + q_3\right] \tag{3}$$

where subscript 0 denotes nominal value at the operating point. Subscripts 1, 2 and 3 denote coefficients of constant impedance, constant current and constant power parts respectively. The static GZIP load model part is contained in output equations of the composite GZIP-IM motor load model.

The dynamic part of the GZIP-IM model is a third-order induction motor model in rotor current form:

$$\frac{di_r}{dt} = \left(B_r - B_s A_s^{-1} A_r\right) i_r + \left(u_r - B_s A_s^{-1} u_s\right) \tag{4}$$

$$\frac{d\omega_r}{dt} = -i_r C_r A_s^{-1} A_r i_r - i_r^T C_r A_s^{-1} u_s - \frac{T_0 \omega_b}{2H}\left(\frac{\omega_r}{\omega_b}\right)^{\beta} \tag{5}$$

where $i_r = \left[i_{dr}, i_{qr}\right]^T$. The detailed expression of the model is described in Appendix A.

By combining the static ZIP part and dynamic third-order induction motor part, a composite GZIP-IM load model of the form (1) is obtained. The state vectors and input-output vectors are represented as follows: $x_r = \left[i_{dr}, i_{qr}, \omega_r\right]^T$, $u = \left[v_{ds}, v_{qs}, \omega\right]^T$, $y = \left[P, Q\right]^T$. Here, the real and reactive power outputs of the GZIP-IM load model are represented by a sum of static ZIP load model output and induction motor output:

$$P = P_{ZIP0}\left[p_1 (V/V_0)^2 + p_2 (V/V_0)^1 + p_3\right] + P_M \tag{6}$$

$$Q = Q_{ZIP0}\left[q_1 (V/V_0)^2 + q_2 (V/V_0)^1 + q_3\right] + Q_M \tag{7}$$

where P_M, Q_M are real and reactive powers consumed by induction motor load and described in (A.7). The model parameter vector to be estimated is defined as: $p = [R_s, R_r, X_s, X_m, X_r, H, T_0, \beta, \omega_{r0}, P_{ZIP0}, p_1, p_2, p_3, Q_{ZIP0}, q_1, q_2, q_3]^T$. The parameter vector is of 17-dimensions with (p_1, q_1), (p_2, q_2), and (p_3, q_3) representing constant impedance, constant current, and constant power, which are associated with the static part of the GZIP-IM model structure. The P_{ZIP0} and Q_{ZIP0} represent the real and reactive power of the static ZIP model at steady state that can be estimated or given by the user. In this paper, the P_{ZIP0}, Q_{ZIP0} are considered a part of the parameters to be estimated. It should be noted that although ω_{r0} is an initial condition of the state equation, it is regarded as a parameter since it is difficult to represent ω_{r0} explicitly by other parameters, input and state variables.

The linearized version of the nonlinear GZIP-IM load model is developed here for modeling the dynamic behaviors of real and reactive powers since the high-order nonlinear dynamic system identification problem is still very challenging. The linearized GZIP-IM load model can be described by:

$$\begin{aligned} \frac{d\Delta x_r}{dt} &= A_{dq}\Delta x_r + B_{dq}\Delta u \\ \Delta y &= C\Delta x_r + D\Delta u \end{aligned} \tag{8}$$

where the point (x_{r0}, u_0) is a steady state satisfying $g(x_{r0}, u_0, p) = 0$, y_0 satisfies $y_0 = h(x_{r0}, u_0, p)$, $\Delta x_r = x_r - x_{r0}$ and $\Delta u = u - u_0$ are state and input increments. $A_{dq} = \partial g / \partial x_r\big|_{x_{r0}, u_0}$, $B_{dq} = \partial g / \partial u\big|_{x_{r0}, u_0}$, $C = \partial h / \partial x_r\big|_{x_{r0}, u_0}$, and $D = \partial h / \partial u\big|_{x_{r0}, u_0}$. The detailed expression of state space matrices, A_{dq}, B_{dq}, C and D is omitted.

It is interesting to note that the coefficients p_3, q_3 representing constant power load of the ZIP load model do not appear in the linearized model, which implies that

p_3, q_3 do not affect estimation results in the linearized model and cannot be estimated independently. The p_3, q_3 are identified via the steady state relations among the input, output and any remaining model parameters.

B. Exponential-Induction Motor Load Model

Exp-IM load model is composed of the static exponential model in parallel with the induction motor. The static part of the Exp-IM load model is represented by an exponential function of bus voltage magnitude as follows:

$$P_{EXP} = P_{EXP0}\left(V/V_0\right)^{Kpv} \tag{9}$$

$$Q_{EXP} = Q_{EXP0}\left(V/V_0\right)^{Kqv} \tag{10}$$

The dynamic part of the Exp-IM load model is the same as that of GZIP-IM load model and is omitted here. Also the state vector and model input vector are identical to those of the GZIP-IM load model. The real and reactive power outputs of the Exp-IM load model are represented by:

$$P = P_{EXP0}\left(V/V_0\right)^{Kpv} + P_M \tag{11}$$

$$Q = Q_{EXP0}\left(V/V_0\right)^{Kqv} + Q_M \tag{12}$$

where P_M, Q_M are real and reactive powers consumed by the induction motor load described in (A.7).

The parameter vector of the Exp-IM load model is defined as:

$p = [R_s, R_r, X_s, X_m, X_r, H, T_0, \beta, \omega_{r0}, P_{EXP0}, K_{pv}, Q_{EXP0}, K_{qv}]^T$

where K_{pv}, K_{qv} are exponents related to real and reactive powers and P_{EXP0}, Q_{EXP0} denote initial real and reactive power portions of the static exponential model part.

The linearized Exp-IM load model can be expressed in the form of (8) and is similar to the linearized GZIP-IM load model. The only difference lies in four elements of the D matrix, which are related to static exponential model power outputs.

C. Z-Induction Motor Load Model

In the Z-IM load model, individual static loads are represented by a single admittance $G_s + jB_s$ connected to the third-order induction motor in parallel. We note that different representations of induction motors are available. In this composite load model representation, internal voltage forms of the induction motor is used [14]. The state and output equations of this model are represented as follows:

$$\begin{cases} T_0'\dfrac{dE'}{dt} = -\dfrac{X}{X'}E' + \dfrac{X-X'}{X'}\cdot V\cdot\cos\delta \\ \dfrac{d\delta}{dt} = \omega - \omega_s - \dfrac{X-X'}{X'}\cdot\dfrac{V\cdot\sin\delta}{T_0'\cdot E'} \\ M\dfrac{d\omega}{dt} = -\dfrac{V\cdot E'\cdot\sin\delta}{X'} - T_m \end{cases} \tag{13}$$

$$\begin{cases} P = G_s V^2 - (VE'/X')\cdot\sin\delta \\ Q = B_s V^2 + V(V - E'\cdot\cos\delta)/X' \end{cases} \tag{14}$$

where E', δ : voltage magnitude and angle behind transient reactance. ω_s, ω : angular velocity of stator and rotor [rad/s], X' : transient reactance, T_0' : transient open-circuit time constant, R_r : rotor resistances (zero stator resistance is assumed), M : motor inertia, T_m : load torque constant. The linearized version of the Z-IM load model in (13), (14) can be similarly derived and the detailed expression is omitted here.

The initial state of (13) is needed to compute output trajectory with given parameters. To obtain the initial state, which is an equilibrium point, we set the derivatives of states of (13) to zero. In order to avoid a numerical problem in calculating $\delta_0 = \sin^{-1}(\arg)/2$ where $\arg = -2X\cdot X'\cdot T_m/((X-X')\cdot V^2)$, we treat initial states $(\delta_0, E_0', \omega_0)$ as unknown parameters to be estimated and steady state conditions are incorporated in the objective function (15) as regularization terms. Hence the number of parameters to be identified increases by three (total 10 parameters) and the parameter vector is redefined as:

$p = [M, T_0', X, X', T_m, E_0', \delta_0, \omega_{r0}, G_s, B_s]^T$.

4. Parameter Estimation Scheme

Once a load model structure is determined, the remaining task of estimating parameter values is formulated as a nonlinear least squares model fitting problem. The error function to be minimized is given as follows:

$$\min_{p\in Z}\varepsilon(p) = \min_{p\in Z}\frac{1}{2}\sum_{k=1}^{N}\left(y(k)-\hat{y}(k)\right)^2 \tag{15}$$

where p denotes a parameter vector to be estimated. N and Z are the total number of samples used for estimation and the feasible parameter space. $y(k)$ and $\hat{y}(k)$ are the measured value and the predicted value of output equation at the k^{th} sample, respectively. As an example, in one set of measurement, the total number of

samples, N was 7680 (=2 sec. × 3840 Hz). To solve the parameter estimation problem (15), the quasi-Newton method is applied. Among the quasi-Newton methods, the Levenberg-Marquardt method is robust and often considered to be a good method for nonlinear least squares problems [15]. Other methods such as the Broyden, Fletcher, Goldfarb, and Shanno (BFGS) are considered reliable and well accepted [16].

It should be noted that ill-conditioned parameter estimation problems can occur. For example if the measurement data is not rich enough to adequately reflect the individual effects of all the parameters or some parameters are structurally unobservable, parameter values may not be reliably estimated. A reliable algorithm has been proposed to identify a subset of parameters that ensures the Jacobian matrix is well-conditioned [17, 18]. The ranking of parameters in the sense of well-condition can be done by performing the subset selection task increasing the number of ill-conditioned parameters from 1 to $m-1$ where m is the dimension of parameter vector p.

In order to solve the ill-conditioned issue, we attempted to estimate all parameters by applying upper and lower bound constraints for parameters first. If a convergence problem occurred in estimation, we then partitioned the parameter vector into a well-conditioned one and ill-conditioned one, and fixed ill-conditioned parameters to their default values. Even though three composite load models in this numerical study have a few ill-conditioned parameters, the numerical convergence problem was not observed during the parameter estimation procedure while some parameters reached their bound values.

With the obtained parameter values, the load model output (response) is simulated and is then compared with the measured output in order to evaluate the performance of the developed load model. To this end, the performance of the developed load model is evaluated using the following relative error ε:

$$\varepsilon = 100 \times \sqrt{\left(\frac{1}{N}\sum_{k=1}^{N}\left(y(k)-\hat{y}(k)\right)^2\right) \Big/ \left(\frac{1}{N}\sum_{k=1}^{N} y(k)^2\right)} \qquad (16)$$

where $y(k)$ and $\hat{y}(k)$ denote the measured and simulated (real or reactive) power, respectively. In this paper, if ε is less than 5%, the composite load model is said to be acceptable.

5. Numerical Studies

In this section, the composite load model of an industrial substation of the Taiwan Power System is developed using the measurement-based approach. The Panchiao substation located in the northern part of Taiwan is an important primary substation supplying power to mostly industrial users. The substation transforms the voltage magnitude of transmission lines from 161 kV to 69 kV via an underload tap changer (ULTC). Eleven sets of measurements are selected from the data-recording system installed at the Panchiao substation. We classified loading conditions into four categories considering month (season) and hour: summer peak (SP), summer medium (SM), summer light (SL), winter light (WL). Table 1 summarizes eleven sets of measurements obtained at the Panchiao substation. These sets of measurements were selected from a larger number of measurements based on several practical guidelines.

Table 1. Test Cases for Composite Load Modeling

Case No.	Time			Loading Condition	Voltage Variation (%)	Real Power Variation (%)
	Month	Day	Hour			
1	8	2	00:24	SL1	5.6	10.4
2	8	2	00:39	SL2	5.5	10.0
3	8	2	01:43	SL3	5.5	10.6
4	8	2	02:39	SL4	5.2	10.5
5	8	9	11:34	SM1	9.1	26.4
6	6	18	11:03	SM2	11.4	12.4
7	6	19	14:38	SP1	16.5	25.8
8	1	11	04:27	WL1	9.0	21.0
9	1	11	06:06	WL2	9.1	21.8
10	1	10	03:08	WL3	12.6	32.5
11	1	6	06:51	WL4	9.8	25.0

As shown in Table 1, the range of voltage magnitude variation of these measurements is between 5.2% and 16.5% with respect to the steady state value of voltage. Real power is in the range of 10.0% ~ 32.5%, which is more significant than voltage variation. The variation of reactive power is generally large (more than 60%), which is partly due to the fact that reactive power is relatively small compared with real power.

We first present the parameter estimation results of the three composite load models using the measurement data of Case 7 in which a large voltage swing occurred. Table 2 lists obtained parameter values and a comparison of estimation results for the GZIP-IM model, Exp-IM model, and Z-IM model respectively. In order to avoid unreasonable parameter values and the ill-conditioned parameter problem, we applied proper lower and upper bound constraints in the estimation.

The estimation results of Case 7 reveal that the GZIP-IM load model gives the best result in modeling real and reactive power behaviors during the disturbance. It is interesting to note that although GZIP-IM and Exp-IM

models have the same third-order induction motor part, some parameters of the induction motor such as X_m, T_0 show quite different values depending on the static part. The estimation results indicate that all three composite load models are well acceptable in modeling both real and reactive power dynamic behaviors.

It can be seen from Table 2 that the Z-IM load model gives inferior results compared with other composite load models in modeling real power behavior while it provides comparable results in modeling reactive power behavior. To illustrate the effectiveness of the proposed composite load model, the simulated real and reactive powers by the GZIP-IM load model are shown in Fig. 2. It is seen from this figure that the GZIP-IM load model can describe both real and reactive power behaviors during disturbance very accurately.

Table 2 Comparison of the parameter estimation using composite models in Case 7

p^*	GZIP-IM	p	EXP-IM	p	Z-IM
R_s	0.1247	R_s	0.1914	M	0.0139
R_r	0.0210	R_r	0.0220	T_0'	0.0963
X_s	0.1056	X_s	0.1682	X	0.2089
X_m	1.0460	X_m	3.0041	X'	0.0446
X_r	0.1423	X_r	0.1194	T_m	8.6157
H	0.0043	H	0.0033	E_0'	1.0750
T_0	1.1120	T_0	0.9068	δ_0	-0.3689
β	2.8888	β	2.9614	ω_{r0}	364.381
ω_{r0}	359.935	ω_{r0}	361.734	G_s	4.1358
P_{ZIP0}	0.8650	P_{EXP0}	0.7550	B_s	2.8004
p_1	0.3631	K_{pv}	1.8444		N/A
p_2	0.4963	Q_{EXP0}	0.3583		N/A
p_3	0.1406	K_{qv}	3.2623		N/A
Q_{ZIP0}	0.0875		N/A		N/A
q_1	0.4313		N/A		N/A
q_2	0.7082		N/A		N/A
q_3	-0.1395		N/A		N/A
$\varepsilon_P(\%)$	0.3241	$\varepsilon_P(\%)$	0.3627	$\varepsilon_P(\%)$	1.1504
$\varepsilon_Q(\%)$	4.1538	$\varepsilon_Q(\%)$	4.4273	$\varepsilon_Q(\%)$	4.4207

p^* : parameter vector

Fig. 3 presents a summary of modeling errors made by these three composite load models on eleven measurement data sets listed in Table 2. We compared the estimation results of composite load models with those of a ZIP-induction motor load model developed in the previous work [6] (denoted by ZIP-IM) and two different third-order induction motor load models: rotor current form and internal voltage form.

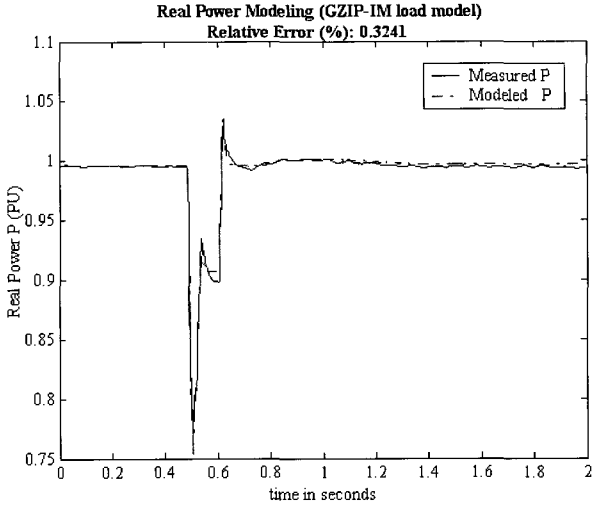

(a) A comparison of real power measurement and modeling

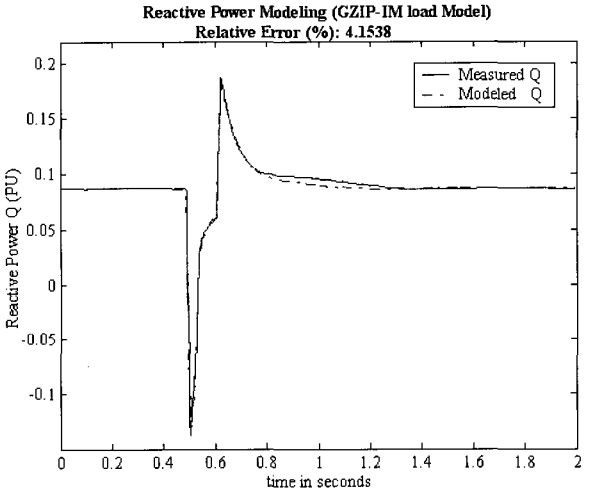

(b) A comparison of reactive power measurement and modeling

Fig. 2 Estimated real and reactive powers using Linearized GZIP-IM Model

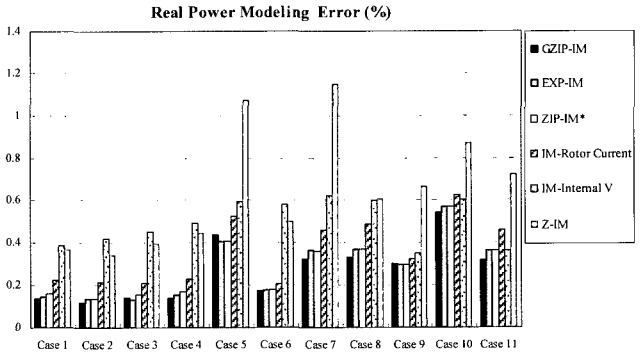

(a) Real power estimation

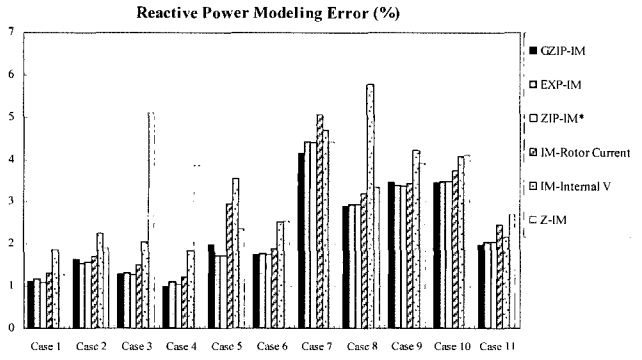

(b) Reactive power estimation

Fig. 3 Comparison of real and reactive power modeling errors by composite load models. Note that ZIP-IM* in the above figure denotes the ZIP-induction motor load model developed in the previous work [6].

From the numerical simulations we have the following observations:

1. Overall, composite load models based on the third-order induction motor model in rotor current form give better results than third-order induction motor load models and Z-IM in modeling both real and reactive power behavior during disturbances.
2. In most cases, GZIP-IM gives the best results among all load models considered in the numerical studies. Z-IM shows inferior results than the induction motor model in internal voltage form in some cases, while its parameter dimension is larger than the induction motor model.
3. Regarding model accuracy, numerical estimation relative errors indicate that all three composite load models are satisfactory in modeling real and reactive power behaviors.
4. We observed that some parameter values of each composite load model are quite different at different loading conditions, which suggests that parameters should be properly updated in order to represent load characteristic at each loading condition.
5. Global optimization techniques deserve to be considered to obtain better solutions since our nonlinear least squares problem has multiple local solutions.

6. Concluding remarks

In this paper, three linear composite load models are developed based on measurement data gathered at different loading conditions in the Taiwan Power System. The estimation performance of each composite load model is compared by eleven measurement data sets at different loading conditions. Numerical considerations for ill-conditioned parameters are addressed to enhance the estimation procedure.

From the numerical studies, we observed that the developed composite load models can accurately model dynamic behaviors of reactive power as well as real power during the disturbance. In particular, composite load models based on the third-order induction motor model in rotor current form provide better results than third-order induction motor load models and the Z-IM load model. Furthermore, we observed that some parameter values of each composite load model are quite dependent on different loading conditions, which suggests that parameters should be properly updated at each loading condition.

Appendix

A. Third-order Induction Motor Model in Rotor Current Form

The dynamic part of the GZIP-IM and Exp-IM load models is represented by the third-order induction motor model in rotor current form. It is known that, in most cases, the changes in stator flux linkages are much faster than the changes in rotor flux linkages. A reduced order induction motor model can be obtained by setting both $d-$ and $q-$axis stator flux changes to zero.

$$\frac{di_{dr}}{dt} = \frac{\omega_b R_s X_m}{\Lambda} i_{ds} - \frac{\omega_b R_r X_{ss}}{\Lambda} i_{dr} - \frac{\omega_r X_m X_{ss}}{\Lambda} i_{qs} + \left(\omega - \frac{\omega_r X_{ss} X_{rr}}{\Lambda}\right) i_{qr} - \frac{\omega_b}{\Lambda} X_m v_{ds} \tag{A.1}$$

$$\frac{di_{qr}}{dt} = \frac{\omega_r X_{ss} X_m}{\Lambda} i_{ds} - \left(\omega - \frac{\omega_r X_{ss} X_{rr}}{\Lambda}\right) i_{dr} + \frac{\omega_b X_m R_s}{\Lambda} i_{qs} - \frac{\omega_b R_r X_{ss}}{\Lambda} i_{qr} - \frac{\omega_b}{\Lambda} X_m v_{qs} \tag{A.2}$$

$$\frac{d\omega_r}{dt} = \frac{\omega_b X_m}{2H}\left(i_{dr} i_{qs} - i_{ds} i_{qr}\right) - \frac{T_0 \omega_b}{2H}\left(\frac{\omega_r}{\omega_b}\right)^{\beta} \tag{A.3}$$

where $\Lambda = X_{ss} X_{rr} - X_m^2$. $X_{ss} = X_s + X_m$. $X_{rr} = X_r + X_m$.

(A.1) ~ (A.3) can be written into a compact form:

$$\frac{di_r}{dt} = \left(B_r - B_s A_s^{-1} A_r\right) i_r + \left(u_r - B_s A_s^{-1} u_s\right) \tag{A.4}$$

$$\frac{d\omega_r}{dt} = -i_r C_r A_s^{-1} A_r i_r - i_r^T C_r A_s^{-1} u_s - \frac{T_0 \omega_b}{2H}\left(\frac{\omega_r}{\omega_b}\right)^{\beta} \tag{A.5}$$

where the vectors in the above compact form are:

$$i_r = \left[i_{dr}, i_{qr}\right]^T, \quad u_s = \begin{bmatrix} v_{ds} \\ v_{qs} \end{bmatrix}, \quad u_r = -\frac{\omega_b}{\Lambda}\begin{bmatrix} X_m v_{ds} \\ X_m v_{qs} \end{bmatrix}$$

$$A_s = \begin{bmatrix} -R_s & \frac{\omega}{\omega_b}X_{ss} \\ -\frac{\omega}{\omega_b}X_{ss} & -R_s \end{bmatrix},\quad A_r = \begin{bmatrix} 0 & \frac{\omega}{\omega_b}X_m \\ -\frac{\omega}{\omega_b}X_m & 0 \end{bmatrix}$$

$$B_r = \begin{bmatrix} -\frac{\omega_b}{\Lambda}R_r X_{ss},\ \omega - \frac{\omega_r}{\Lambda}X_{ss}X_{rr} \\ -\left(\omega - \frac{\omega_r}{\Lambda}X_{ss}X_{rr}\right),\ -\frac{\omega_b}{\Lambda}R_r X_{ss} \end{bmatrix}$$

$$C_r = \frac{(X_m \cdot \omega_b)}{2H}\begin{bmatrix} 0 & 1 \\ -1 & 0 \end{bmatrix}$$

(A.4) and (A.5) can be rewritten into the following compact form:

$$\dot{x}_r = g(x_r, u, p) \tag{A.6}$$

The real power P and Q consumed by induction motor loads can be computed as follows:

$$\begin{aligned} P_M &= v_{ds}i_{ds} + v_{qs}i_{qs} = u_s^T i_s = u_s^T\left(-A_s^{-1}A_r i_r - A_s^{-1}u_s\right) \\ Q_M &= v_{qs}i_{ds} - v_{ds}i_{qs} = \begin{bmatrix} v_{qs} - v_{ds} \end{bmatrix} i_s = \begin{bmatrix} v_{qs} - v_{ds} \end{bmatrix}\left(-A_s^{-1}A_r i_r - A_s^{-1}u_s\right) \end{aligned} \tag{A.7}$$

where $i_s = -A_s^{-1}A_r i_r - A_s^{-1}u_s$

The outputs of the GZIP-IM model and Exp-IM model can be rewritten into the following compact form:

$$y = h(x_r, u, p) \tag{A.8}$$

Hence, the state dynamics and outputs of the induction motor load can be described by equations (A.4), (A.5) and (A.8). Thus, a steady-state point, say (x_{r0}, u_0) of the load model must satisfy the following steady state condition.

$$y_0 = h(x_{r0}, u_0, p) \tag{A.9}$$

$$0 = g(x_{r0}, u_0, p) \tag{A.10}$$

Acknowledgements

This work was supported in part by the Taiwan Power Company and by the Electric Power Research Institute (EPRI). Dr. Byoung-Kon Choi was supported in part by a Korea Research Foundation Grant funded by the Korean Government (MOEHRD) (KRF-2004-214-D00081).

References

[1] CIGRE Task Force 38.02.05, "Load Modeling and Dynamics", Electra, May 1990.

[2] *IEEE Recommended Practice for Excitation System Models for Power System Stability Studies*, IEEE Standard 421. 5-1992.

[3] *IEEE Standard Definitions for Excitation Systems and Synchronous Machines*, IEEE Standard 421. 1-1986.

[4] IEEE Task Force on Load Representation for Dynamic Performance, "Bibliography on load models for power flow and dynamic performance simulation," *IEEE Trans. Power Syst.*, vol. 10, no. 1, pp. 523-538, Feb. 1995.

[5] Dingguo Chen, Ronald R. Mohler, "Neural-network-based load modeling and its use in voltage stability analysis," *IEEE Trans. Control Systems Technology*, vol. 11, no. 11, pp. 460-470, Jul. 2003.

[6] H.-D. Chiang et al., "Development of a dynamic ZIP-motor load model from on-line field measurements", *International Journal of Electrical Power & Energy Systems*, vol. 19, no. 7, pp. 459-468, 1997.

[7] C.-Y. Chiou, C.-H. Huang, H.-D. Chiang, J.-C. Wang, "Development of a microprocessor-based transient data recording system for load behavior analysis", *IEEE Trans. Power Syst.*, vol. 8, no. 1, pp. 16-22, 1993.

[8] C.-J. Lin, Y.-T. Chen, H.-D. Chiang, and J.-C. Wang, "Dynamic load models in power systems using the measurement approach," *IEEE Trans. Power Syst.*, vol. 8, no. 1, pp. 309-315, Feb. 1993.

[9] J.-C. Wang, H.-D. Chiang, C.-L. Chang, and A.-H. Liu, "Development of a frequency-dependent composite load model using the measurement approach," *IEEE Trans. Power Syst.*, vol. 9, no. 3, pp. 1546-1556, Aug. 1994.

[10] Y. Baghzouz, Craig Quist, "Composite load model derivation from recorded field data," in *Proc. IEEE PES 1999 Winter Meeting, vol. 1*, pp. 713 – 718, 31 Jan.-4 Feb. 1999.

[11] Ju, P., Handschin, E., Karlsson, D, "Nonlinear dynamic load modeling: model and parameter estimation," *IEEE Trans. Power Syst.*, vol. 11, no. 4, pp. 1689 - 1697, Nov. 1996.

[12] Wen-Shiow Kao, Chia-Tien Lin, Chiang-Tsang Huang, Yung-Tien Chen, Chiew-Yann Chiou, "Comparison of simulated power system dynamics applying various load models with actual recorded data", *IEEE Trans. Power Syst.*, vol. 9, no. 1, pp. 248 – 254, Feb. 1994.

[13] Keyhani, A.; Lu, W.; Heydt, G.T., "Composite neural network load models for power system stability analysis", *IEEE PES Power Systems Conference and Exposition*, 2004, vol. 2, pp. 1159 – 1163, Oct. 2004.

[14] S. Ahmed-Zaid, M. Taleb, "Structural Modeling of

Small and Large Induction Machines Using Integral Manifolds", *IEEE Transactions on Energy Conversion*, vol. 6, no. 3, pp. 529 – 535, Sep. 1991.

[15] R. Fletcher, *Practical Methods of Optimization*, Second Edition, John Wiley & Sons, New York, 1987.

[16] L.G. Dias, M.E. El-Hawary, "Nonlinear parameter estimation experiments for static load modeling in electric power systems," *IEE Proc.* vol. 136, Pt. C, no. 2, pp. 68-77, Mar. 1998.

[17] M. Burth, G. C. Verghese, and M. Velez-Reyes, "Subset selection for improved parameter estimation in on-line identification of a synchronous generator," *IEEE Trans. Power Syst.*, vol. 14, no. 1, pp. 218-225, Feb. 1999.

[18] P. M. Frank, *Introduction to System Sensitivity Theory*. New York: Academic Press, 1978.

[19] P. Kundur, Power System Stability and Control, McGraw-Hill, Inc., 1994.

Byoung-Kon Choi received his B.S, M.S., and Ph.D. degrees in Electrical Engineering from Yonsei University, Seoul, Korea in 1994, 1996, and 2000, respectively. He worked for LG CNS as a Senior Consultant from 2000 to 2003. He is currently working at Cornell University as a Post-Doc. Associate.

Hsiao-Dong Chiang received his Ph.D. degree in Electrical Engineering and Computer Sciences from the University of California at Berkeley in 1986. He is currently a Professor of Electrical and Computer Engineering at Cornell University, Ithaca, NY.

Yinhong Li received her B.S. and Ph.D. degrees in Electrical Engineering from Huazhong University of Science and Technology, Wuhan, China in 1998 and 2004, respectively. She is currently working at Cornell University as a Post-Doc. Associate.

Yung-Tien Chen received his diploma in Electrical Engineering from the Taipei Institute of Technology in 1965. He is currently Director of the System Planning Department at the Taiwan Power Company.

Der-Hua Huang is a Deputy Director in the System Planning Department at the Taiwan Power Company.

Mark G. Lauby received his BEE and MSEE degrees from the University of Minnesota in 1980 and 1989 respectively. From 1980 to 1987, he worked with the Mid-Continent Area Power Pool. Since 1987 he has been with Electric Power Research Institute (EPRI), & EPRI International, Palo Alto, California in various positions. He currently is the Director, Power Delivery & Markets.